INDENTER GEOMETRY EFFECTS ON THE MEASUREMENT OF MECHANICAL PROPERTIES BY NANOINDENTATION WITH SHARP INDENTERS

1996

T.Y. TSUI*, W.C. OLIVER**, and G.M. PHARR*

* Department of Materials Science, Rice University, 6100 Main St., Houston, TX 77005
** Nanoinstruments Inc., 1001 Larson Drive, Oak Ridge, TN 37830

ABSTRACT

The measurement of mechanical properties by nanoindentation methods is most often conducted using indenters with the Berkovich geometry (a triangular pyramid) or with a sphere. These indenters provide a wealth of information, but there are certain circumstances in which it would be useful to make measurements with indenters of other geometries. We have recently explored how the measurement of hardness and elastic modulus can be achieved using sharp indenters other than the Berkovich. Systematic studies in several materials were conducted with a Vickers indenter, a conical indenter with a half-included tip angle of 70.3°, and the standard Berkovich indenter. All three indenters are geometrically similar and have nominally the same area-to-depth relationship, but there are distinct differences in the behavior of each. Here, we report on the application of these indenters in the measurement of hardness and elastic modulus by nanoindentation methods and some of the difficulties that occur.

INTRODUCTION

The measurement of mechanical properties such as hardness, H, and elastic modulus, E, by nanoindentation methods has been conducted largely with indenters having the Berkovich or spherical geometries [1-4]. The Berkovich indenter, a three-sided pyramid with the same area-to-depth ratio as the Vickers indenter commonly used in microindentation testing, is useful in experiments where full plasticity is needed at very small penetration depths, such as the measurement of hardness of very thin films and surface layers [1,2]. The spherical indenter, on the other hand, is useful when purely elastic contact or the transition from elastic to plastic contact is of interest [3,4].

Of the many sharp indenters used for microhardness testing, the Berkovich has proven the most useful in nanoindentation work. This is because the three sided pyramidal geometry of the Berkovich naturally terminates at a point, thus facilitating the grinding of diamonds which maintain their sharpness to very small scales. Berkovich tip defects, as characterized by the effective tip radius, are frequently less than 50 nm in many of the better diamonds. For the Vickers indenter, on the other hand, it is more difficult to maintain geometric similarity at such small scales because the square-based pyramidal geometry does not terminate at a point but rather at a "chisel" edge. The conical indenter is the most difficult to grind, and as a result, conical diamonds often have severe tip rounding.

Nevertheless, there are certain circumstances in which it may be useful to make nanoindentation property measurements with a Vickers or a conical indenter. The Vickers, for example, may be useful in measuring the properties of single crystals with 4-fold symmetry, or to directly compare hardnesses obtained in nanoindentation experiments with conventional Vickers microhardness results. In addition, the Vickers indenter is the primary indenter used in measuring the fracture toughness of brittle materials by the indentation cracking method [5]. The conical indenter has advantages when one wishes to avoid deformation phenomena caused by the sharp edges of the Berkovich and Vickers indenters, e.g., when cracking is to be avoided in brittle materials or when large strain gradients around the circumference of the contact complicate the understanding of indentation phenomena. The conical indenter is also more amenable to analysis than the Berkovich or Vickers; virtually all modelling of indentation contact by sharp indenters uses the conical geometry [6], and with very few exceptions [7], most finite element simulations of indentation by sharp indenters have used the conical geometry to take advantage of the axial symmetry [8-10].

MASTER

For these reasons, an elementary study to examine the problems that are encountered in using Vickers and conical indenters in nanoindentation testing was undertaken. The study focused on three sharp diamonds: a Berkovich. a Vickers, and a conical diamond with a half-included tip angle of 70.3°. All three have the same nominal area-to-depth relationship, thus removing this factor as a variable in the study and thereby simplifying the understanding of results. Here we present a select set of results for four materials chosen to represent the behavior of metals and ceramics. A much larger number of materials were studied, but space considerations prohibit us from including all of them. A more complete report is in preparation [11].

EXPERIMENTAL PROCEDURE

The four materials examined in the study were fused quartz, a well-annealed aluminum single crystal, a mechanically polished specimen of polycrystalline gold (large grains), and a single crystal of (001) sapphire. The first two materials are used as standards in nanoindentation testing for the determination of indenter area functions, and the latter two are included to illustrate specific points that help in understanding the indentation behavior of the three diamonds. Indentations were made in each of the materials at a variety of loads, and the indentation load-displacement behavior was analyzed to determine H and E using a variation on the method of Oliver and Pharr [2].

The variation was developed to account for recent observations that the machine compliance in a nanoindentation experiment may not be constant for a given machine, but rather may depend on how the specimen is mounted and the way in which the mount is secured to the nanoindentation system. As a result, a single, specimen-independent machine compliance cannot be used in precision work. This is not an important consideration for materials and experimental conditions for which the contact stiffness is small (i.e. contact stiffnesses much less than the machine stiffness), but can lead to significant errors in some experimental situations. The errors become particularly important when making large indentations (loads of 50 mN or more) in very soft materials like well-annealed aluminum. Since aluminum is a material we use as a standard in making area function determinations, we have altered the procedure by which the area function is measured to account for the influences of the mount on the machine compliance.

To briefly describe the procedure, a number of indentations are made to various peak loads up to 300 mN, and the areas, A, of the largest indentations are measured optically. The highest load indentations are large enough that their areas can be measured with accuracies of about ±5%. Using Young's modulus E=70 GPa and Poisson's ratio $v=0.34$ (the values for polycrystalline aluminum), the machine compliance, C_m, is then found from :

$$C = C_T - \frac{\sqrt{\pi}}{2} \frac{(1 - v^2)}{E} \frac{1}{\sqrt{A}} \qquad (1)$$

where C_T is the total compliance measured in the experiment (see [2] for the origin of this equation). Using this value for C_m to evaluate the load-displacement data obtained at other loads, an area function is then established by solving Eqn.1 for A. Unfortunately, aluminum is not a good calibration material for indentation depths smaller than 500 nm because of scatter in the data, possibly caused by the oxide film. For this reason, the small-depth portion of the area function is established in separate experiments conducted on fused quartz, which can be conveniently indented to depths ranging from 5 to 1500 nm. The machine compliance for the fused quartz experiments is determined by a trial and error procedure in which a value of C_m is sought which, when applied to Eqn.1 and using E=72 GPa and $v=0.17$ (the values for fused quartz), gives contact areas which match those of the aluminum data in the region of overlap (500 nm<h_c<1500 nm). After combining the two data sets, curve fitting procedures are used to produce an area function which applies over the range 20-7000 nm. This technique is used in preference to the procedure outlined in [2] because the latter involves an extrapolation which can lead to errors in C_m.
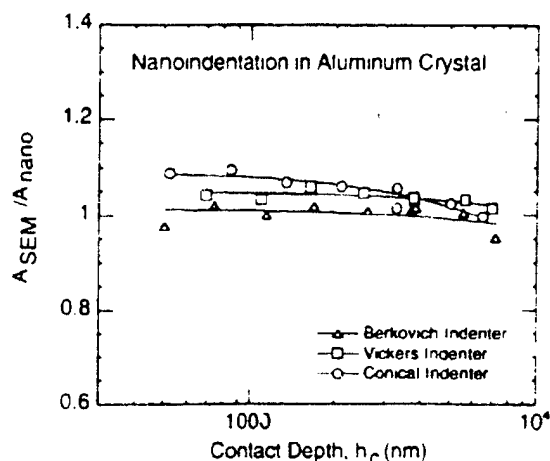
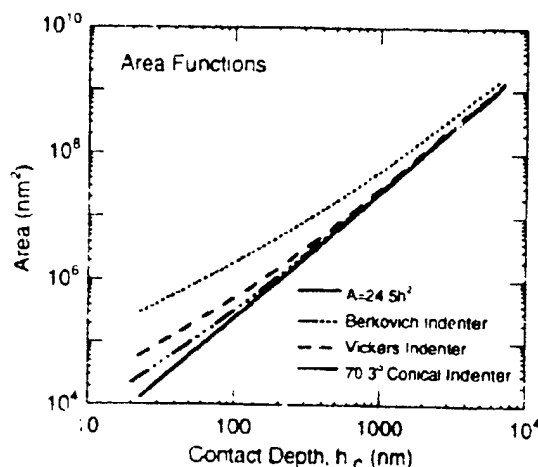Fig.1. A comparison of nanoindentation areas with SEM measurements for Al.

Fig.2. Experimentally determined area functions for each of the indenters.

RESULTS AND DISCUSSION

The area function determination procedure just described was used in the current study to establish the area function of each of the three indenters. To check how well the procedure works, Figure 1 presents results for indentations in aluminum which compare the areas predicted from analysis of the nanoindentation load-displacement data, A_{nano}, to areas measured by direct examination of scanning electron microscopy (SEM) images, A_{SEM}. The measurements are limited to the indentation depths greater than 500 nm due to difficulties in obtaining clear, measurable images at smaller depths. Over the range of depths examined, the SEM areas for the Berkovich and Vickers indentations deviate from predictions of the area function by no more than 5%. For the conical indenter, the deviation is slightly larger, but only at small depths where it is difficult to make good measurements. Thus, the procedure for deriving the area functions appears to work reasonably well for each three indenters, at least over the range of indentation sizes which are convenient to check in the SEM.

The complete area functions are shown in Figure 2, where they have been evaluated over their range of applicability, i.e., $h_c = 20$ to 7000 nm. Also shown in the figure is the ideal area function, $A=24.5h^2$. The ideal area function is that which all three diamonds would exhibit if they were ground to perfect geometric form. The plot shows that while the geometry of the Berkovich indenter is in closest agreement with ideal geometry, the 70.3° cone shows significant deviations over most of the applicable contact range. The deviations are consistent with the notion that the 70.3° cone is very blunt and possibly more sphe.e-like than sharp at the scales of interest in this study. The Vickers indenter lies somewhere in between. As will be shown shortly, deviations from perfect geometry play an important role in understanding the results of the nanoindentation hardness measurements.

Measurements of elastic modulus and hardness for each of the four materials by each of the three diamond indenters are summarized in Figure 3. The elastic moduli are shown in the plots in the left-hand column. Not surprisingly, the moduli for aluminum and fused quartz are very close to the expected values, E = 70 GPa and 72 GPa, irrespective of indenter geometry. This, of course, must be the case, since these values were used as input in the procedure by which the area functions were established. The true test comes from the other two materials, gold and sapphire. For the gold data, all three indenters give approximately the same value for E. Furthermore, the measured modulus is independent of indentation depth and has a value which compares quite favorably with the known polycrystalline gold value, E=80 GPa [12]. Comparison of the sapphire data with actual values for E is a little more difficult because the modulus of sapphire varies depending on crystallographic orientation in the range 400-500 GPa [2]. However, inspection of the data in Figure 3 shows that all three indenters give depth-independent elastic moduli which fall generally in this range. Thus, based on these limited
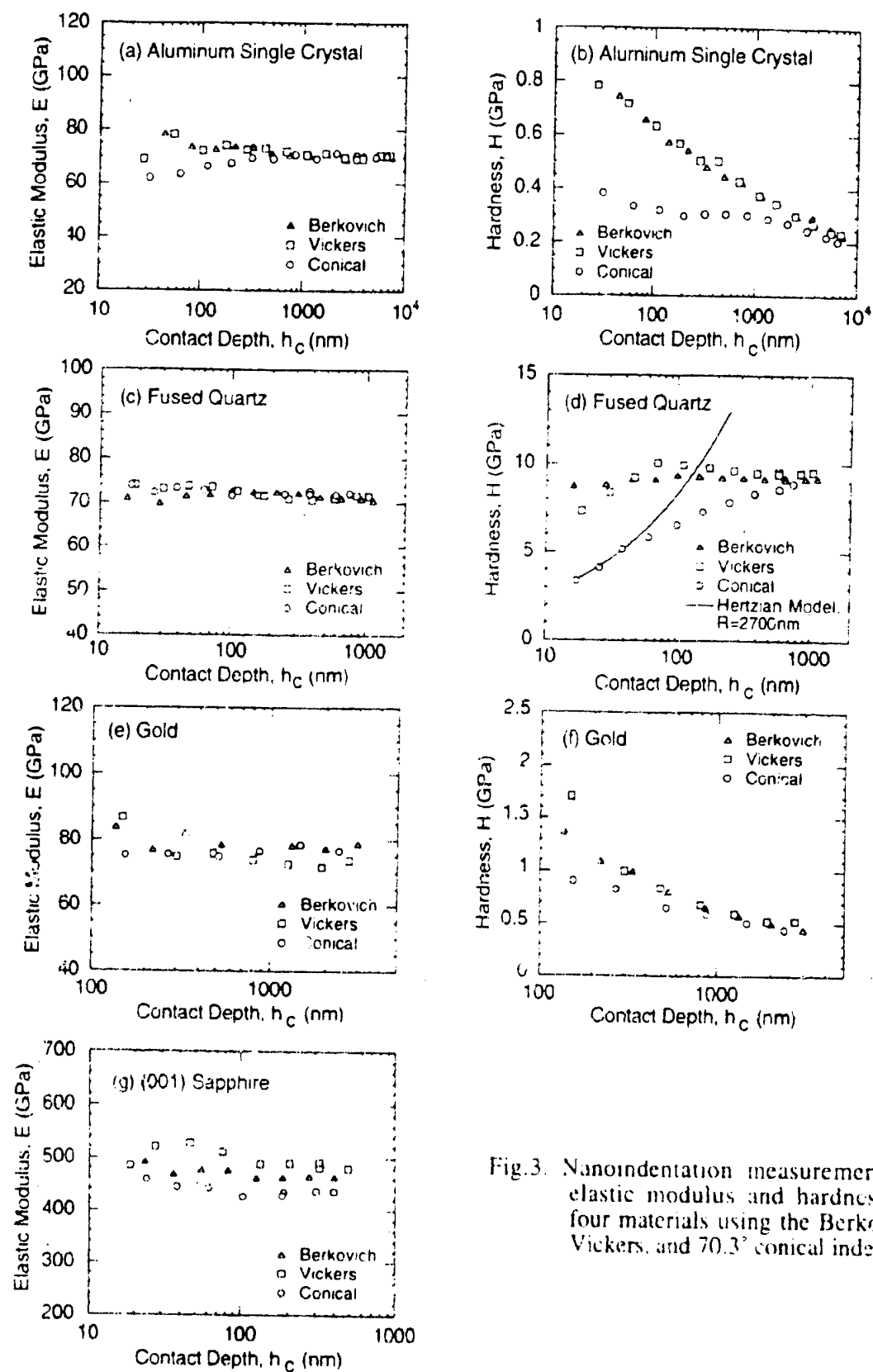
(a) Aluminum Single Crystal

Elastic Modulus, E (GPa)

▲ Berkovich
□ Vickers
○ Conical

Contact Depth, h_c (nm)

(b) Aluminum Single Crystal

Hardness, H (GPa)

▲ Berkovich
□ Vickers
○ Conical

Contact Depth, h_c (nm)

(c) Fused Quartz

Elastic Modulus, E (GPa)

▲ Berkovich
□ Vickers
○ Conical

Contact Depth, h_c (nm)

(d) Fused Quartz

Hardness, H (GPa)

▲ Berkovich
□ Vickers
○ Conical
—— Hertzian Model, R=270nm

Contact Depth, h_c (nm)

(e) Gold

Elastic Modulus, E (GPa)

▲ Berkovich
□ Vickers
○ Conical

Contact Depth, h_c (nm)

(f) Gold

Hardness, H (GPa)

▲ Berkovich
□ Vickers
○ Conical

Contact Depth, h_c (nm)

(g) (001) Sapphire

Elastic Modulus, E (GPa)

▲ Berkovich
□ Vickers
○ Conical

Contact Depth, h_c (nm)

Fig.3. Nanoindentation measurements of elastic modulus and hardness for four materials using the Berkovich, Vickers, and 70.3° conical indenters.

observations, it appears that nanoindentation measurement of elastic modulus using sharp indenters other than the Berkovich is indeed possible. It should be noted, however, that accurate measurements can be achieved only when the deviations from the ideal indenter geometry are taken into account. Had the ideal area function been used, different results would have been obtained.

The hardness data shown in the right hand column of Figure 3 show some peculiar and interesting behaviors. For example, the aluminum data at the top of the column shows a significant indentation size effect (ISE) for the Berkovich and Vickers indenters, but not for the conical indenter. Based on SEM measurement of the actual contact areas (Fig.1), it is clear that the indentation size effect is real and not just an artifact of the data analysis procedures (at least for contact depths greater than 500 nm). Collectively, these data suggest that the ISE in aluminum may be caused by localized plastic deformation at the edges of the indenter. A model based on this concept has been developed by Ma and Clarke [13]. The gold hardness data exhibit behavior similar to that of the aluminum, with the exception that the hardnesses measured with the conical indenter are not quite as flat.

The hardness behavior of the fused quartz specimen is quite different. For this material, the Berkovich and Vickers indenters give very similar, depth-independent hardnesses, but there is a large increase in hardness with increasing depth for the data obtained with the conical indenter. Thus, it appears that there is a completely different indentation size effect in this material, one which runs contrary to most ISE observations reported in the literature (the usual observation is increasing hardness with decreasing depth), and one which is unique to the conical indenter. However, shortly we will show that this behavior is not real, but results from a transition from purely elastic to elastic/plastic deformation caused by the bluntness of the conical indenter.

The key to understanding the behavior of the fused quartz data was unveiled while testing the (001) sapphire. Hardness data for this material are presented in Figure 4, where the individual data points, rather than the averages plotted in previous graphs, are shown. A curious feature in the data is the division of the Vickers hardnesses at depths less than 100 nm into 2 distinct groups, one considerably higher than the other. Examination of the individual load-displacement curves revealed that the higher data points correspond to purely elastic indentation contact, as evidenced by loading and unloading curves which perfectly retrace themselves. For each of the lower data points, on the other end, there was a plastic pop-in event similar to that reported by Page et al. [14]. Subsequent investigation of the data for the conical indenter revealed the same behavior, with the transition from purely elastic to elastic/plastic deformation occurring at slightly larger contact depths. Purely elastic indentation contact is promoted by tip blunting. The transition is not observed in the Berkovich data, presumably because the Berkovich is considerably sharper than the other two indenters.

The observation of purely elastic contact at small indentation depths for the Vickers and conical indenters has important consequences for the interpretation of hardnesses measured ... nanoindentation experiments. Specifically, the hardness, H=P/A, obtained by applying the Oliver/Pharr analysis procedure to nanoindentation load-displacement data is not the traditional hardness based on the residual area of the hardness impression, but a different hardness based on the area of contact at peak load. In soft materials, these two hardnesses are essentially the same, but for hard materials they can be different, particularly when deformation during indentation is mostly elastic and recoverable. To amplify on this point, note that in the limit of purely elastic contact, the conventional hardness rises without bound, while that derived by the Oliver/Pharr procedure has a finite value. In fact, assuming that the blunting of indenters can be characterized by assigning a radius of curvature to the tip, one can compute from Hertzian contact theory what the Oliver/Pharr hardness should be for purely elastic contact. A simple analysis yields:

$$ H = \frac{4\sqrt{2}}{3\pi} \frac{E}{(1-v^2)} \left(\frac{h_c}{R} \right)^{1/2} \tag{2} $$

where R is the effective radius of curvature of the tip.

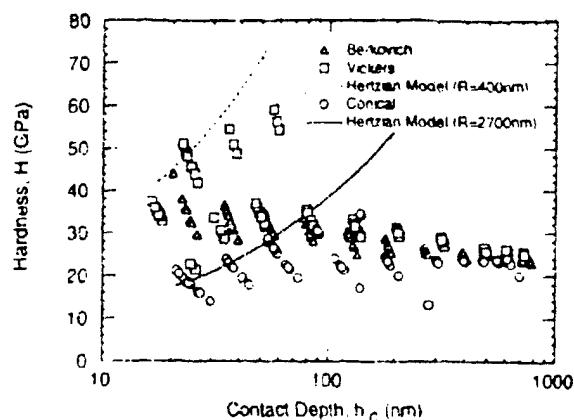To show that this phenomenon is indeed the source of the decrease in hardness at low loads

Fig.4. Nanoindentation hardness measurement of (001) sapphire using the Berkovich, Vickers , and 70.3° conical indenters.

in sapphire, Hertzian analysis was used to extract an effective tip radius from the low-load, reversible load-displacement data obtained for both the conical and Vickers indenters. The tip radii were found to be R=400 nm for the Vickers and R=2700 nm for the cone. Using these radii in Eqn. 2 along with reasonable estimates of the elastic constants, predictions based on the Oliver/Pharr definition of hardness and Hertzian contact theory are included in Figure 4, where it is seen that relatively good agreement is obtained with the experimental data points corresponding to purely elastic contact. Using R=2700 nm, the predictions of Eqn. 2 have also been computed for comparison to the conical indentation of fused quartz and are included in hardness data of Figure 3. Once again, there is relatively good agreement with the low-load data.

CONCLUSIONS

1. Using careful techniques to establish the area function of the indenter, it is possible to use conical and Vickers indenters in the measurement of elastic modulus by nanoindentation methods, even though these indenters suffer more from tip defects than the Berkovich indenter used more commonly in nanoindentation testing.

2. The tip defect confuses the interpretation of hardnesses measured by nanoindentation methods, since there is a change in the mode of deformation from purely elastic at low loads to elastic/plastic at high loads. This phenomena is more important in hard materials such as ceramics and glasses than it is in soft metals.

ACKNOWLEDGMENTS

REFERENCES

1. G.M. Pharr and W.C. Oliver. MRS Bull. XVII, 28 (1992).
2. W.C. Oliver and G.M. Pharr, j Mater. Res. 7, 1564 (1992).
3. J.S. Field and M.V. Swain, J. Mater. Res. 8, 297 (1993).
4. J.S. Field and M.V. Swain, J. Mater. Res. 10, 101 (1995).
5. G.R. Anstis, P. Cnantikul, B R.Lawn, and D.B.Marshall, J. Am. Cer. Soc. 63, 574 (1980).
6. K.L. Johnson, Contact Mechanics (Cambridge University Press, Cambridge, UK, 1985).
7. A.E. Giannakopoulos, P.L. Larsson & R Vestergaard, Int. J. Solids Struct. 31, 2679 (1994).
8. A.K. Bhattacharya and W.D. Nix, Int. J. Solids Structures 24, 1287 (1988).
9. T.A. Larsen and J.C Simo, J. Mater. Res. 7, 618 (1992).
10. A. Bolshakov, W C Oliver, and G.M. Pharr, J. Mater. Res. 11, 760 (1996).
11. T.Y. Tsui and G.M. Pharr, in preparation.
12. G. Simmons and H. Wang, Single Crystal Elastic Constants and Calculated Aggregate Properties: A Handbook, 2nd ed. (The MIT Press, Cambridge, MA, 1971).
13. Q. Ma and D.R. Clarke, J. Mater. Res. 10, 853 (1995).
14. T.F. Page, W.C. Oliver and C.J. McHargue, J. Mater. Res. 7, 450 (1992).

observations, it appears that nanoindentation measurement of elastic modulus using sharp indenters other than the Berkovich is indeed possible. It should be noted, however, that accurate measurements can be achieved only when the deviations from the ideal indenter geometry are taken into account. Had the ideal area function been used, different results would have been obtained.

The hardness data shown in the right hand column of Figure 3 show some peculiar and interesting behaviors. For example, the aluminum data at the top of the column shows a significant indentation size effect (ISE) for the Berkovich and Vickers indenters, but not for the conical indenter. Based on SEM measurement of the actual contact areas (Fig.1), it is clear that the indentation size effect is real and not just an artifact of the data analysis procedures (at least for contact depths greater than 500 nm). Collectively, these data suggest that the ISE in aluminum may be caused by localized plastic deformation at the edges of the indenter. A model based on this concept has been developed by Ma and Clarke [13]. The gold hardness data exhibit behavior similar to that of the aluminum, with the exception that the hardnesses measured with the conical indenter are not quite as flat.

The hardness behavior of the fused quartz specimen is quite different. For this material, the Berkovich and Vickers indenters give very similar, depth-independent hardnesses, but there is a large increase in hardness with increasing depth for the data obtained with the conical indenter. Thus, it appears that there is a completely different indentation size effect in this material, one which runs contrary to most ISE observations reported in the literature (the usual observation is increasing hardness with decreasing depth), and one which is unique to the conical indenter. However, shortly we will show that this behavior is not real, but results from a transition from purely elastic to elastic/plastic deformation caused by the bluntness of the conical indenter.

The key to understanding the behavior of the fused quartz data was unveiled while testing the (001) sapphire. Hardness data for this material are presented in Figure 4, where the individual data points, rather than the averages plotted in previous graphs, are shown. A curious feature in the data is the division of the Vickers hardnesses at depths less than 100 nm into 2 distinct groups, one considerably higher than the other. Examination of the individual load-displacement curves revealed that the higher data points correspond to purely elastic indentation contact, as evidenced by loading and unloading curves which perfectly retrace themselves. For each of the lower data points, on the other end, there was a plastic pop-in event similar to that reported by Page et al. [14]. Subsequent investigation of the data for the conical indenter revealed the same behavior, with the transition from purely elastic to elastic/plastic deformation occurring at slightly larger contact depths. Purely elastic indentation contact is promoted by tip blunting. The transition is not observed in the Berkovich data, presumably because the Berkovich is considerably sharper than the other two indenters.

The observation of purely elastic contact at small indentation depths for the Vickers and conical indenters has important consequences for the interpretation of hardnesses measured in nanoindentation experiments. Specifically, the hardness, $H=P/A$, obtained by applying the Oliver/Pharr analysis procedure to nanoindentation load-displacement data is not the traditional hardness based on the residual area of the hardness impression, but a different hardness based on the area of contact at peak load. In soft materials, these two hardnesses are essentially the same, but for hard materials they can be different, particularly when deformation during indentation is mostly elastic and recoverable. To amplify on this point, note that in the limit of purely elastic contact, the conventional hardness rises without bound, while that derived by the Oliver/Pharr procedure has a finite value. In fact, assuming that the blunting of indenters can be characterized by assigning a radius of curvature to the tip, one can compute from Hertzian contact theory what the Oliver/Pharr hardness should be for purely elastic contact. A simple analysis yields:

$$ H = \frac{4\sqrt{2}}{3\pi} \frac{E}{(1-v^2)} \left(\frac{h}{R} \right)^{1/2} \qquad (2) $$

where R is the effective radius of curvature of the tip.

To show that this phenomenon is indeed the source of the decrease in hardness at low loads

DISCLAIMER